



# Synthesis and characterization of rhodium(I) 2-methylcupferrate complexes and their kinetic behaviour in iodomethane oxidative addition

Stefan Warsink, Fanuel G. Fessha, Walter Purcell, Johan A. Venter\*

Department of Chemistry, University of the Free State, PO Box 339, Bloemfontein 9300, South Africa

## ARTICLE INFO

### Article history:

Received 19 November 2012

Accepted 4 December 2012

### Keywords:

Oxidative addition

Rhodium

Cupferrate

Iodomethane

Kinetics

## ABSTRACT

A number of substituted monocarbonyl complexes  $[\text{Rh}(\text{MeCupf})(\text{CO})(\text{PR}_3)]$  (where R = Ph, *p*-MeOph, *p*-Tol, *o*-Tol and Cy, MeCupf = *N*-nitroso-*N*-(2-methylphenyl)hydroxylaminato bidentate ligand) have been prepared from  $[\text{Rh}(\text{MeCupf})(\text{CO})_2]$  and identified by IR, UV/visible and NMR techniques. The kinetics and mechanism for the oxidative addition of iodomethane to  $[\text{Rh}(\text{MeCupf})(\text{CO})(\text{PR}_3)]$  complexes have been investigated through the variation of steric and electronic effects of the phosphine ligands, as well as through varying the solvent and temperature. The  $\text{Rh}^{\text{III}}$ -alkyl complex was the primary species formed as a result of oxidative addition, followed by a consecutive slower formation of the  $\text{Rh}^{\text{III}}$ -acyl species by carbonyl-insertion. A detailed mechanism is discussed.

© 2012 Elsevier B.V. All rights reserved.

## 1. Introduction

The synthesis of rhodium organometallic complexes in our laboratory is covered in a large number of articles [1–4]. A significant number of these studies involve the synthesis of  $[\text{Rh}(\text{LL}'\text{-BID})(\text{CO})(\text{PPh}_3)]$  (where LL'-BID = monoanionic bidentate ligands containing different donor atoms L and L') and other relevant complexes. These complexes were synthesised to study the electronic and steric influence of the different bidentate (LL') and monodentate ligands on the rate of substitution and oxidative addition reactions, as well as to evaluate the complexes as possible catalysts in organic synthesis. One of these complexes,  $[\text{Rh}(\text{Cupf})(\text{CO})(\text{PPh}_3)]$  (Cupf = *N*-nitroso-*N*-phenylhydroxylaminato bidentate ligand) indicated that it has the tendency to form a very stable 5-coordinated complex as was illustrated by the characterisation of  $[\text{Rh}(\text{Cupf})(\text{CO})(\text{PPh}_3)_2]$  [2]. The oxidative addition reaction between  $[\text{Rh}(\text{Cupf})(\text{CO})(\text{PPh}_3)]$  and iodomethane [1c] also clearly indicated the catalytic participation of a five-coordinated solvent-stabilized complex,  $[\text{Rh}(\text{Cupf})(\text{CO})(\text{PPh}_3)(\text{S})]$ . Another interesting result from this study was the formation of a *cis*- $[\text{Rh}(\text{Cupf})(\text{CO})(\text{PPh}_3)(\text{CH}_3)(\text{I})]$  oxidative addition complex compared to the final *trans* product for the  $\text{H}_3\text{C}-\text{Rh}-\text{I}$  moiety for a large number of those complexes such as  $[\text{Rh}(\text{ox})(\text{CO})(\text{PPh}_3)(\text{CH}_3)(\text{I})]$  [3] and  $[\text{Rh}(\text{dmavk})(\text{CO})(\text{PPh}_3)(\text{CH}_3)(\text{I})]$  (ox = oxine, dmavk = dimethylaminovinylketone) [4]. This

paper describes the synthesis and characterisation of a series of rhodium complexes containing a methyl substituted cupferrate derivative, MeCupf, as bidentate ligand. It also describes the oxidative addition of iodomethane to these complexes and the analysis of its kinetics.

## 2. Experimental

### 2.1. General procedures and instrumentation

Rhodium(III) chloride (Aldrich), 2-nitrotoluene (Merck), *n*-butyl nitrite (Merck), triphenylphosphine (Merck) and iodomethane (Merck) were used as purchased. Organic solvents used were distilled prior to use and water was double distilled.

Infrared spectra of the solids were collected in the range of 2300–550  $\text{cm}^{-1}$  using a Digilab Merlin 3.0 spectrophotometer. NMR spectra were obtained with Bruker 300 and 600 MHz spectrophotometers.  $^1\text{H}$  NMR data are listed in the order: chemical shift ( $\delta$ , reported in ppm and referenced to the residual solvent peak of  $\text{CD}_2\text{Cl}_2$  [ $\delta = 5.32$  ppm]), multiplicity, coupling constant ( $J$ , in Hz), number of hydrogens, assignment. Hydrogen decoupled  $^{13}\text{C}$  NMR data are listed in the order: chemical shift ( $\delta$ , reported in ppm and referenced to the residual solvent peak of  $\text{CD}_2\text{Cl}_2$ ), multiplicity, coupling constant ( $J$ , in Hz), assignment. Hydrogen and carbon decoupled  $^{31}\text{P}$  NMR data are listed in the order: chemical shift ( $\delta$ , reported in ppm and referenced to triphenylphosphine oxide [ $\delta = 29.9$  ppm]), multiplicity, coupling constant ( $J$ , in Hz). Positive

\* Corresponding author. Tel.: +27 514013336; fax: +27 514446384.  
E-mail address: [venterja@ufs.ac.za](mailto:venterja@ufs.ac.za) (J.A. Venter).

chemical shifts ( $\delta$ ) are denoted for high-frequency shifts relative to the solvent ( $^{13}\text{C}$ ) or  $\text{H}_3\text{PO}_4$  capillary ( $^{31}\text{P}$ ).

All kinetic measurements were carried out in air and all solvents were pre-dried over aluminium oxide and distilled. UV/visible spectra were collected on a Varian Cary 50 double-beam spectrophotometer equipped with temperature cell regulator (accurate within 0.1 °C) in a  $1.000 \pm 0.001$  cm quartz cuvette. Infrared spectra of liquids were recorded in dry organic solvents (toluene or dichloromethane) in a NaCl cell in the range 2100–1600  $\text{cm}^{-1}$  using a Digilab Merlin 3.0 Spectrophotometer equipped with a temperature cell regulator (accurate within 0.3 °C). Iodomethane is highly volatile and the solutions were prepared in a fume hood and used immediately after preparation. The Cary 50 double-beam spectrophotometer was initially used to verify the stability of the  $[\text{Rh}(\text{MeCupf})(\text{CO})(\text{PR}_3)]$  complexes in different solvents. Suitable wavelengths were consequently selected to study the reaction between  $[\text{Rh}(\text{MeCupf})(\text{CO})(\text{PR}_3)]$  complexes and iodomethane in the different solvents used. Typical complex concentrations were  $1.7 \times 10^{-4}$  M for UV/visible and 0.02 M for IR kinetic measurements. Iodomethane concentrations were varied between 0.2 and 1 M thus ensuring good pseudo-first-order plots of  $\ln(A_t - A_\infty)$  vs time where  $A_t$  and  $A_\infty$  are the absorbencies at time  $t$  and infinity, respectively. The mathematical calculations for the kinetic investigations were performed using the Scientist programme [5]. Some of the reactions were performed using both the IR and UV/visible spectrophotometer to correlate the different reactions with all the physical changes during the reactions.

## 2.2. Synthesis of biscarbonyl (*O,O'*-(*N*-nitroso-*N*-oxido-(2-tolyl)-amine))rhodium(I)

$\text{RhCl}_3 \cdot x\text{H}_2\text{O}$  (300 mg, 1.12 mmol) was heated in DMF (25 ml) at 180 °C to produce tetracarbonyl-dichloro-dirhodium(I) [6]. 2-Methylcupferrate (190 mg, 1.26 mmol) was added slowly to the cooled solution, after which ice water was added dropwise to precipitate the complex. The product was obtained after filtration and drying *in vacuo* as a brick-red solid in a yield of 84%.  $^1\text{H}$  NMR (300 MHz,  $\text{CD}_2\text{Cl}_2$ , 25 °C):  $\delta$  7.54–7.48 (2H, m, Cupf), 7.42–7.36 (m, 2H, Cupf), 2.37 (3H, s,  $\text{CH}_3$ ).  $^{13}\text{C}\{^1\text{H}\}$  NMR (75 MHz,  $\text{CD}_2\text{Cl}_2$ , 25 °C):  $\delta$  184.6 (d,  $^1J_{\text{Rh}-\text{C}} = 74.7$  Hz, CO), 184.4 (d,  $^1J_{\text{Rh}-\text{C}} = 73.1$  Hz, CO), 137.8 (1-Cupf-C), 133.6 (2-Cupf-C), 131.8, 131.3, 126.8, 124.9 (4Cupf-CH), 18.0 ( $\text{CH}_3$ ). IR  $\nu_{\text{max}}/\text{cm}^{-1}$ : 2063, 2087 (CO). Analysis calculated for  $\text{C}_9\text{H}_7\text{N}_2\text{O}_4\text{Rh}$  (310.07): C, 34.86; H, 2.28; N, 9.03. Found: C, 34.66; H, 2.73; N, 9.27.

## 2.3. Synthesis of $[\text{Rh}(\text{MeCupf})(\text{CO})(\text{PR}_3)]$ complexes

$[\text{Rh}(\text{MeCupf})(\text{CO})_2]$  (0.252 g, 0.814 mmol) was dissolved in 5 ml acetone. The phosphine ligand (0.235 g, 0.895 mmol) was added slowly to the solution. Ice water was then added dropwise to the solution to precipitate the complex. The solid was then filtered and dried at room temperature.

### 2.3.1. Carbonyl triphenylphosphine (*O,O'*-(*N*-nitroso-*N*-oxido-(2-tolyl)-amine))rhodium(I), $[\text{Rh}(\text{MeCupf})(\text{CO})(\text{PPh}_3)]$

The product was obtained as a yellow solid in a yield of 94%.  $^1\text{H}$  NMR (300 MHz,  $\text{CD}_2\text{Cl}_2$ , 25 °C):  $\delta$  7.75–7.25 (m, 19H, Ph, Cupf), 2.41 (s, 3H,  $\text{CH}_3$ , minor isomer), 2.19 (s, 3H,  $\text{CH}_3$ , major isomer).  $^{13}\text{C}\{^1\text{H}\}$  NMR major isomer (151 MHz,  $\text{CD}_2\text{Cl}_2$ , 25 °C):  $\delta$  190.4 (dd,  $^1J_{\text{Rh}-\text{C}} = 76.8$  Hz,  $^2J_{\text{P}-\text{C}} = 25.2$  Hz, CO), 138.7 (s, 1-Cupf-C), 134.1 (d,  $^2J_{\text{P}-\text{C}} = 11.9$  Hz, *o*-Ph-CH), 133.1 (s, 2-Cupf-C), 131.9 (d,  $^1J_{\text{P}-\text{C}} = 9.8$  Hz, *i*-Ph-C), 131.6 (s, 6-Cupf-CH), 130.6 (d,  $^4J_{\text{P}-\text{C}} = 2.2$  Hz, *p*-Ph-CH), 130.2 (s, 4-Cupf-CH), 128.3 (d,  $^3J_{\text{P}-\text{C}} = 7.6$  Hz, *m*-Ph-CH), 126.4, 124.6 (2s, 3-Cupf-CH, 5-Cupf-CH), 18.4 (s, Cupf- $\text{CH}_3$ ).  $^{31}\text{P}\{^1\text{H}, ^{13}\text{C}\}$  NMR (121 MHz,  $\text{CD}_2\text{Cl}_2$ , 25 °C):  $\delta$  48.25 (d,  $^1J_{\text{Rh}-\text{P}}$

$\text{P} = 174.2$  Hz, minor isomer), 47.33 (d,  $^1J_{\text{Rh}-\text{P}} = 170.7$  Hz, major isomer). IR  $\nu_{\text{max}}/\text{cm}^{-1}$ : 1982 (CO). Analysis calculated for  $\text{C}_{26}\text{H}_{22}\text{N}_2\text{O}_3\text{PRh}$  (544.34): C, 57.37; H, 4.07; N, 5.15. Found: C, 57.83; H, 4.39; N, 5.26.

### 2.3.2. Carbonyl tri-(4-tolyl)-phosphine (*O,O'*-(*N*-nitroso-*N*-oxido-(2-tolyl)-amine))rhodium(I), $[\text{Rh}(\text{MeCupf})(\text{CO})(\text{P}(p\text{-Tol})_3)]$

The product was obtained as a yellow solid in a yield of 78%.  $^1\text{H}$  NMR (300 MHz,  $\text{CD}_2\text{Cl}_2$ , 25 °C):  $\delta$  7.6–7.45 (m, 6H, aryl-H), 7.45–7.3 (m, 4H, Cupf-H), 7.3–7.2 (m, 6H, aryl-H), 2.43 (s, 3H, aryl- $\text{CH}_3$ , minor isomer), 2.41 (s, 3H, aryl- $\text{CH}_3$ , major isomer), 2.37 (s, 3H, Cupf- $\text{CH}_3$ , minor isomer), 2.21 (s, 3H, Cupf- $\text{CH}_3$ , major isomer).  $^{13}\text{C}\{^1\text{H}\}$  NMR major isomer (151 MHz,  $\text{CD}_2\text{Cl}_2$ , 25 °C):  $\delta$  190.5 (dd,  $^1J_{\text{Rh}-\text{C}} = 77.0$  Hz,  $^2J_{\text{P}-\text{C}} = 25.3$  Hz, CO), 141.0 (s, *p*-aryl-C), 138.8 (s, 1-Cupf-C), 133.9 (d,  $^2J_{\text{P}-\text{C}} = 11.9$  Hz, *o*-aryl-CH), 133.1 (s, 2-Cupf-C), 131.7 (d,  $^1J_{\text{P}-\text{C}} = 4.0$  Hz, *i*-aryl-C), 131.6 (s, 6-Cupf-CH), 130.1 (s, 4-Cupf-CH), 129.0 (d,  $^3J_{\text{P}-\text{C}} = 11.0$  Hz, *m*-aryl-CH), 126.3 (5-Cupf-CH), 124.6 (3-Cupf-CH), 21.1 (s, aryl- $\text{CH}_3$ ), 18.4 (s, Cupf- $\text{CH}_3$ ).  $^{31}\text{P}\{^1\text{H}, ^{13}\text{C}\}$  NMR (121 MHz,  $\text{CD}_2\text{Cl}_2$ , 25 °C):  $\delta$  46.22 (d,  $^1J_{\text{Rh}-\text{P}} = 173.2$  Hz, minor isomer), 44.93 (d,  $^1J_{\text{Rh}-\text{P}} = 169.4$  Hz, major isomer). IR  $\nu_{\text{max}}/\text{cm}^{-1}$ : 1969 (CO). Analysis calculated for  $\text{C}_{29}\text{H}_{28}\text{N}_2\text{O}_3\text{PRh}$  (586.42): C, 59.29; H, 4.98; N, 4.77. Found: C, 59.14; H, 5.36; N, 5.16.

### 2.3.3. Carbonyl tri-(4-methoxyphenyl)-phosphine (*O,O'*-(*N*-nitroso-*N*-oxido-(2-tolyl)-amine))rhodium(I), $[\text{Rh}(\text{MeCupf})(\text{CO})(\text{P}(p\text{-MeOPh})_3)]$

The product was obtained as a yellow solid in a yield of 93%.  $^1\text{H}$  NMR (300 MHz,  $\text{CD}_2\text{Cl}_2$ , 25 °C):  $\delta$  7.65–7.45 (m, 6H, aryl-H), 7.40–7.25 (m, 4H, Cupf-H), 7.05–6.90 (m, 6H, aryl-H), 3.88 (s, 9H, OCH<sub>3</sub>, minor isomer), 3.85 (s, 9H, OCH<sub>3</sub>, major isomer), 2.41 (s, 3H, Cupf- $\text{CH}_3$ , minor isomer), 2.22 (s, 3H, Cupf- $\text{CH}_3$ , major isomer).  $^{13}\text{C}\{^1\text{H}\}$  NMR major isomer (151 MHz,  $\text{CD}_2\text{Cl}_2$ , 25 °C):  $\delta$  190.6 (dd,  $^1J_{\text{Rh}-\text{C}} = 77.5$  Hz,  $^2J_{\text{P}-\text{C}} = 25.3$  Hz, CO), 161.5 (s, *p*-aryl-C), 138.8 (s, 1-Cupf-C), 135.5 (d,  $^2J_{\text{P}-\text{C}} = 13.3$  Hz, *o*-aryl-CH), 133.1 (s, 2-Cupf-C), 131.6 (d,  $^1J_{\text{P}-\text{C}} = 3.6$  Hz, *i*-aryl-C), 130.1 (s, 6-Cupf-CH), 126.3 (s, 4-Cupf-CH), 124.6, 124.1 (2 s, 3-Cupf-CH, 5-Cupf-CH), 113.8 (d,  $^3J_{\text{P}-\text{C}} = 13.3$  Hz, *m*-aryl-CH), 55.3 (s, OCH<sub>3</sub>), 18.6 (s, Cupf- $\text{CH}_3$ ).  $^{31}\text{P}\{^1\text{H}, ^{13}\text{C}\}$  NMR (121 MHz,  $\text{CD}_2\text{Cl}_2$ , 25 °C):  $\delta$  44.00 (d,  $^1J_{\text{Rh}-\text{P}} = 172.9$  Hz, minor isomer), 42.84 (d,  $^1J_{\text{Rh}-\text{P}} = 169.0$  Hz, major isomer). IR  $\nu_{\text{max}}/\text{cm}^{-1}$ : 1965 (CO). Analysis calculated for  $\text{C}_{29}\text{H}_{28}\text{N}_2\text{O}_6\text{PRh}$  (634.42): C, 54.81; H, 4.60; N, 4.41. Found: C, 55.35; H, 4.75; N, 4.49.

### 2.3.4. Carbonyl tri-(2-tolyl)-phosphine(*O,O'*-(*N*-nitroso-*N*-oxido-(2-tolyl)-amine))rhodium(I), $[\text{Rh}(\text{MeCupf})(\text{CO})(\text{P}(o\text{-Tol})_3)]$

The product was obtained as a yellow solid in a yield of 84%.  $^1\text{H}$  NMR (300 MHz,  $\text{CD}_2\text{Cl}_2$ , 25 °C):  $\delta$  7.9–7.8 (m, 3H, 6-tolyl-H), 7.45–7.35 (m, 4H, Cupf-H, tolyl-H), 7.35–7.2 (m, 9H, Cupf-H, tolyl-H), 2.4 (s, 9H, tolyl- $\text{CH}_3$ ), 2.13 (s, 3H,  $\text{CH}_3$ , minor isomer), 1.95 (s, 3H,  $\text{CH}_3$ , major isomer).  $^{13}\text{C}\{^1\text{H}\}$  NMR major isomer (151 MHz,  $\text{CD}_2\text{Cl}_2$ , 25 °C):  $\delta$  190.1 (dd,  $^1J_{\text{Rh}-\text{C}} = 79.1$  Hz,  $^2J_{\text{P}-\text{C}} = 23.4$  Hz, CO), 142.8 (d,  $^2J_{\text{P}-\text{C}} = 8.7$  Hz, 6-aryl-CH), 138.6 (s, 1-Cupf-C), 135.0 (br s, 2-aryl-C), 133.1 (s, 2-Cupf-C), 131.9 (d,  $^1J_{\text{P}-\text{C}} = 8.1$  Hz, 1-aryl-C), 131.6 (s, 6-Cupf-CH), 130.8 (s, 5-aryl-CH), 130.0 (s, 4-Cupf-CH), 129.1 (s, 3-aryl-CH), 126.3 (s, 5-Cupf-CH), 125.7 (s, 4-aryl-CH), 124.4 (s, 3-Cupf-CH), 23.3 (d,  $^3J_{\text{P}-\text{C}} = 6.6$  Hz, aryl- $\text{CH}_3$ ), 18.2 (s, Cupf- $\text{CH}_3$ ).  $^{31}\text{P}\{^1\text{H}, ^{13}\text{C}\}$  NMR (121 MHz,  $\text{CD}_2\text{Cl}_2$ , 25 °C):  $\delta$  43.43 (d,  $^1J_{\text{Rh}-\text{P}} = 173.7$  Hz, minor isomer), 41.14 (d,  $^1J_{\text{Rh}-\text{P}} = 171.9$  Hz, major isomer). IR  $\nu_{\text{max}}/\text{cm}^{-1}$ : 1970 (CO). Analysis calculated for  $\text{C}_{29}\text{H}_{28}\text{N}_2\text{O}_3\text{PRh}$  (586.42): C, 59.29; H, 4.98; N, 4.77. Found: C, 55.43; H, 4.91; N, 4.39.

### 2.3.5. Carbonyl tricyclohexylphosphine (*O,O'*-(*N*-nitroso-*N*-oxido-(2-tolyl)-amine))rhodium(I), $[\text{Rh}(\text{MeCupf})(\text{CO})(\text{PCy}_3)]$

The product was obtained as a pink solid in a yield of 82%.  $^1\text{H}$  NMR (300 MHz,  $\text{CD}_2\text{Cl}_2$ , 25 °C):  $\delta$  7.60–7.50 (m, 2H, Cupf-H), 7.50–

7.30 (m, 2H, Cupf-H), 2.39 (s, 3H, CH<sub>3</sub>, minor isomer), 2.34 (s, 3H, CH<sub>3</sub>, major isomer), 2.10–2.00 (m, 3H, 1-Cy-H), 1.90–1.45 (m, 12H, 2-Cy-H, 6-Cy-H), 1.40–1.10 (m, 18H, 3-Cy-H, 4-Cy-H, 5-Cy-H). <sup>13</sup>C {<sup>1</sup>H} NMR major isomer (151 MHz, CD<sub>2</sub>Cl<sub>2</sub>, 25 °C): δ 191.5 (dd, <sup>1</sup>J<sub>Rh-C</sub> = 77.7 Hz, <sup>2</sup>J<sub>P-C</sub> = 23.2 Hz, CO), 139.2 (s, 1-Cupf-C), 133.2 (s, 2-Cupf-C), 131.5 (s, 6-Cupf-CH), 130.1 (s, 4-Cupf-CH), 126.4 (5-Cupf-CH), 124.8 (3-Cupf-CH), 34.8 (d, <sup>1</sup>J<sub>P-C</sub> = 25.7 Hz, 1-Cy-CH), 30.0 (s, 3-Cy-CH<sub>2</sub>, 5-Cy-CH<sub>2</sub>), 27.5 (d, <sup>2</sup>J<sub>P-C</sub> = 4.0 Hz, 2-Cy-CH<sub>2</sub>, 6-Cy-CH<sub>2</sub>), 26.4 (s, 4-Cy-CH<sub>2</sub>), 18.6 (s, Cupf-CH<sub>3</sub>). <sup>31</sup>P{<sup>1</sup>H, <sup>13</sup>C} NMR (121 MHz, CD<sub>2</sub>Cl<sub>2</sub>, 25 °C): δ 62.43 (d, <sup>1</sup>J<sub>Rh-P</sub> = 164.0 Hz, minor isomer), 61.82 (d, <sup>1</sup>J<sub>Rh-P</sub> = 161.6 Hz, major isomer). IR ν<sub>max</sub>/cm<sup>-1</sup>: 1956 (CO). Analysis calculated for C<sub>26</sub>H<sub>40</sub>N<sub>2</sub>O<sub>3</sub>PRh (562.49): C, 55.52; H, 7.17; N, 4.98. Found: C, 55.91; H, 7.34; N, 4.62.

### 3. Results and discussion

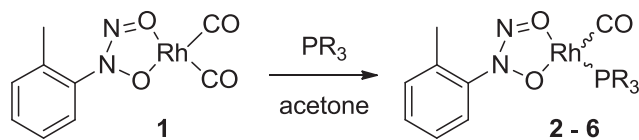
#### 3.1. Synthesis of rhodium(I) complexes

Using 2-methyl-substituted cupferron as ligand [7], the biscarbonyl rhodium(I) complex **1** was synthesized using the well-known dinuclear precursor [Rh-μ-Cl(CO)<sub>2</sub>]<sub>2</sub> (Scheme 1) [6].

This complex was isolated in a yield of 84% and has characteristic signals in the IR spectrum for the two carbonyl ligands at 2063 and 2087 cm<sup>-1</sup>. This complex was then reacted with differently substituted phosphines to generate sterically and electronically varying monocarbonyl complexes in good to excellent yields (Scheme 2) [8].

From <sup>1</sup>H, <sup>13</sup>C and <sup>31</sup>P NMR it appeared that the substitution reaction shown in Scheme 2 did not proceed with a high selectivity as two structural isomers were routinely obtained in an approximate ratio of 1:2, irrespective of the phosphine ligand used. This shows that the difference in *trans*-influence of the donor atoms of the cupferrate ligand is not significant enough as to achieve selective substitution of a specific carbonyl ligand. When the results for this substituted ligand were compared with those for the parent ligand, it appeared that no NMR data were reported. Therefore, the parent [Rh(Cupf)(CO)(PPh<sub>3</sub>)] complex was synthesized according to the same procedure as for complexes **2–6**. It appeared that under these conditions two isomers were also formed. From this it can be concluded that this behaviour is typical of the rhodium cupferrate complexes investigated, and results pertaining to the *trans*-influence of the two oxygen donors drawn solely from crystallographic studies should be critically evaluated. All efforts to separate the two complexes did not yield a single product in any significant yield. Based on the small electronic difference between the two isomers, very similar behaviour (to the point of equal) is expected in kinetic experiments.

Characteristic for the complexes **2–6** is the occurrence of only one carbonyl stretching signal in the IR spectra, although two signals would be expected. Apparently, the resolution of the spectra is not so high as to show the small difference in electronic density imparted on the carbonyl ligand by the two different oxygen donors. Furthermore, the occurrence of a single carbonyl signal indicates that only one of the carbonyl ligands was substituted by a phosphine ligand. The carbonyl *trans* to the donating moiety with the largest *trans*-influence is expected to be substituted in the



**Scheme 2.** Ligand substitution to introduce different phosphine ligands. R = Ph (**2**), 4-MePh (**3**), 4-OMePh (**4**), 2-MePh (**5**), Cy (**6**).

major isomer, as its bond to the rhodium is labilized most, although the reverse has also been observed for electron-withdrawing phosphite ligands which are sterically less demanding [9]. However, this does not need to be an electronic effect, as the crystallization of the minor isomer is a realistic option. In the case of the unsubstituted cupferrate ligand, the nitroso-oxygen has the highest *trans*-influence; the methyl-substituent on the phenyl-ring is not expected to change this to a significant degree.

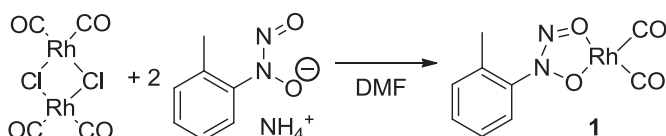
The pK<sub>a</sub> values of the free phosphine ligands are frequently used as an index of basicity and are proportional to the electron donating ability of the phosphine. According to Table 1, pK<sub>a</sub> values for the different phosphine ligands increase from PPh<sub>3</sub> to PCy<sub>3</sub> which indicates that there is an increase in electron donating capability (strong basicity) of the substituent on the tertiary phosphine from PPh<sub>3</sub> to PCy<sub>3</sub>.

The corresponding values of the CO vibrations from the IR spectra are also given in Table 1. It can be seen that the value observed for the carbonyl ligand in the IR decreases with increasing phosphine pK<sub>a</sub>. This can be explained by the electron-donating properties of the phosphine ligands, which correlates with the pK<sub>a</sub> value. The higher this value, the more nucleophilic the phosphorus centre, which increases the electron density on the rhodium upon coordination. This in turn reduces the bond order in the CO ligand through an increase in π-backbonding, leading to a lower wavenumber for its vibration in the infrared. However, this trend does not hold for complex **5**, bearing the tris(*o*-tolyl)phosphine ligand. The pK<sub>a</sub> value would suggest that a ν<sub>CO</sub> lying between that of complex **2** and **3** should be observed. Instead, the observed value is almost identical to that of complex **4**, bearing the much more nucleophilic tris(*p*-anisyl)phosphine. The discrepancy arises from the fact that not only electronic factors are important in this ligand series. For the phosphine ligands in complex **5** and **6**, the steric component is substantially different than for those in the complexes **2–4**. This does not change the nucleophilicity of the ligand, but it does influence the coordination environment around the rhodium centre to a significant degree. The influence of the cupferrate substituent can also be gauged by comparison with literature values for rhodium(I) complexes bearing the unsubstituted cupferrate [1c]. This comparison shows that the 2-methylcupferrate ligand induces ν<sub>CO</sub> signals to be observed at slightly lower wavenumbers than the parent ligand. This effect is expected to have a mostly electronic nature, caused by the electron donating methyl substituent.

**Table 1**

Carbonyl IR-signals of **2–6**, pK<sub>a</sub>-values of the free phosphine and the cone angles of the different phosphines as defined by Tolman [10].

Complex	PR <sub>3</sub>	pK <sub>a</sub>	ν <sub>CO</sub> (cm <sup>-1</sup> )	Cone angle (°)
<b>2</b>	PPh <sub>3</sub>	2.73	1982	145
<b>3</b>	P(4-MePh) <sub>3</sub>	3.84	1970	145
<b>4</b>	P(4-OMePh) <sub>3</sub>	4.57	1964	145
<b>5</b>	P(2-MePh) <sub>3</sub>	3.08	1965	194
<b>6</b>	PCy <sub>3</sub>	9.65	1954	170



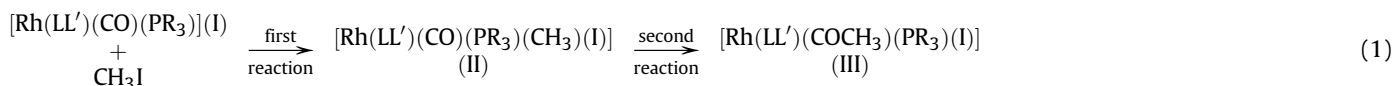
**Scheme 1.** Synthesis of [Rh(MeCupf)(CO)<sub>2</sub>].

### 3.2. Kinetic studies

The stability of the  $[\text{Rh}(\text{MeCupf})(\text{CO})(\text{PPh}_3)]$  complex in different solvents was verified in solutions of acetone, chloroform, acetonitrile, ethyl acetate, methanol and benzene. The solutions were monitored with UV/visible spectroscopy for a number of hours. No significant amount of decomposition took place under the selected experimental conditions for at least 13 h. The reaction between  $[\text{Rh}(\text{MeCupf})(\text{CO})(\text{PR}_3)]$  and iodomethane gave a broad absorption maximum in the 340–450 nm region and all kinetic measurements were done at a particular maximum absorption (Fig. 1).

### 3.3. Reaction mechanism

The IR and UV/visible spectra clearly indicate that all the different  $\text{Rh}^{\text{I}}\text{--MeCupf}$  complexes react with iodomethane. These results also point to the formation of the  $\text{Rh}^{\text{III}}\text{--alkyl}$  product in the first reaction (oxidative addition) and the subsequent acyl formation in the second reaction as indicated in equation (1).



The  $\text{Rh}(\text{I})\text{--CO}$  stretching frequency at about  $1978\text{ cm}^{-1}$  for (I) disappears with the simultaneous appearance of the  $\text{Rh}^{\text{III}}\text{--CO}$  peak at about  $2057\text{ cm}^{-1}$  for (II). The peak formation at  $1722\text{ cm}^{-1}$  is indicative of acyl formation for (III) (Fig. 2). Another important aspect of all the IR spectra is the complete disappearance of the  $\text{Rh}^{\text{I}}\text{--CO}$  peak which points to a large forward reaction (large equilibrium constant) with little or no reverse reaction.

The kinetic study of the reaction between  $[\text{Rh}(\text{MeCupf})(\text{CO})(\text{PR}_3)]$  and different iodomethane concentrations showed a significant intercept which could not be attributed to the reverse reaction. This intercept can only be attributed to the involvement of solvent molecules in the overall reaction. Using this information the following mechanism is proposed for the reaction between  $[\text{Rh}(\text{MeCupf})(\text{CO})(\text{PR}_3)]$  and iodomethane (Scheme 3).

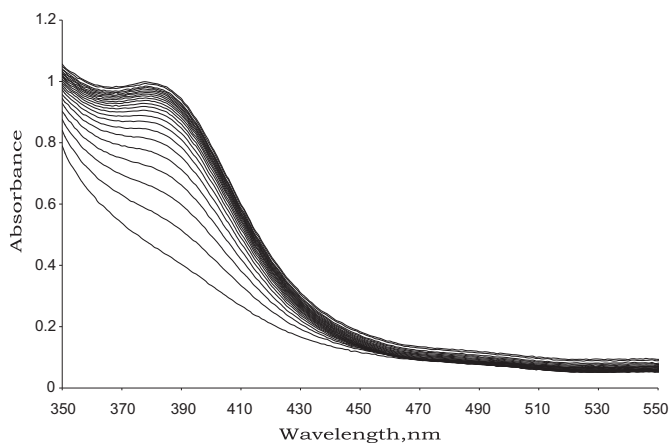


Fig. 1. Visible spectra (4 min interval) for the reaction between  $[\text{Rh}(\text{MeCupf})(\text{CO})(\text{PPh}_3)]$  and iodomethane in acetone at  $25.0\text{ }^\circ\text{C}$ ,  $[\text{Rh}] = 1.7 \times 10^{-4}\text{ M}$ .

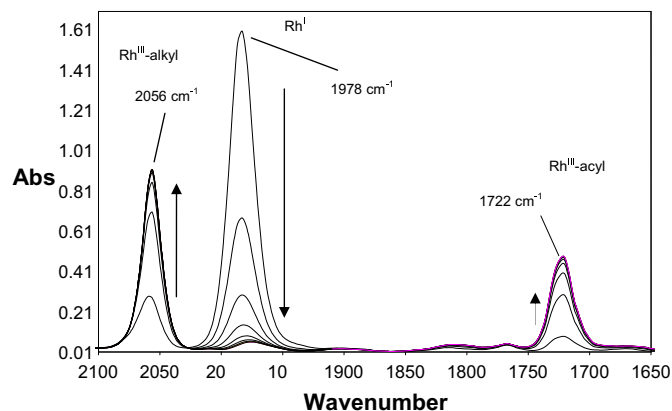


Fig. 2. Consecutive IR scans (4 min intervals) for the oxidative addition of  $[\text{Rh}(\text{MeCupf})(\text{CO})(\text{PPh}_3)]$  with iodomethane in chloroform at  $25.0\text{ }^\circ\text{C}$ ,  $[\text{Rh}] = 0.02\text{ M}$ ,  $[\text{CH}_3\text{I}] = 0.2\text{ M}$ .

### 3.4. Rate laws

The rate law for the alkyl formation reaction, assuming that  $k_3$  is a fast reaction, is given by equation (2).

$$-d[\text{Rh}^{\text{I}}]/dt = (k_1[\text{CH}_3\text{I}] + k_2[\text{S}])[\text{Rh}(\text{MeCupf})(\text{CO})(\text{PR}_3)] \quad (2)$$

Equation (2) simplifies to equation (3) under pseudo-first-order conditions with  $[\text{Rh}(\text{MeCupf})(\text{CO})(\text{PR}_3)] \ll [\text{CH}_3\text{I}]$ .

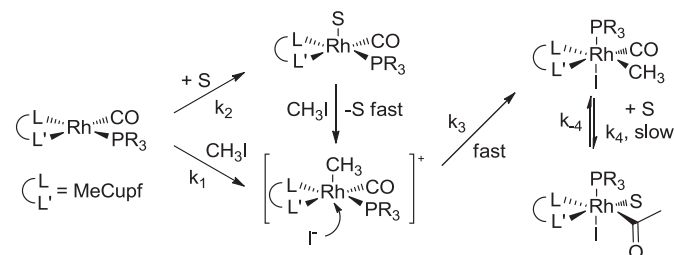
$$k_{\text{obs}} = k_1[\text{CH}_3\text{I}] + k_2[\text{S}] = k_1[\text{CH}_3\text{I}] + k_2' \quad (3)$$

The rate law for the acyl formation (final step in Scheme 3) is given by equation (4).

$$\begin{aligned} & [\text{Rh}(\text{MeCupf})(\text{COCH}_3)(\text{PR}_3)(\text{I})(\text{S})]/dt \\ &= k_4[\text{Rh}(\text{MeCupf})(\text{CO})(\text{PR}_3)(\text{CH}_3)(\text{I})][\text{S}] \\ &+ k_{-4}[\text{Rh}(\text{MeCupf})(\text{CO})(\text{CH}_3)(\text{PR}_3)(\text{I})] \end{aligned} \quad (4)$$

Hence,

$$R = (k_4[\text{S}] + k_{-4})[\text{Rh}(\text{MeCupf})(\text{CO})(\text{PR}_3)(\text{CH}_3)(\text{I})] \quad (5)$$



Scheme 3. Mechanism for the oxidative addition reaction between  $[\text{Rh}(\text{MeCupf})(\text{CO})(\text{PR}_3)]$  and iodomethane.

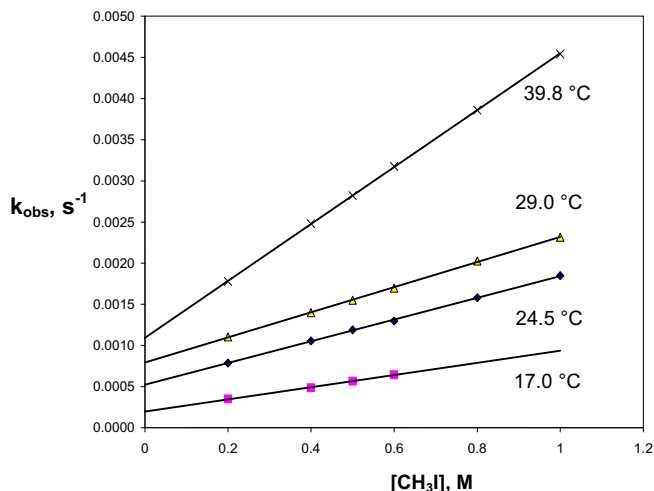


Fig. 3. Kinetic results for the oxidative addition between  $[\text{Rh}(\text{MeCupf})(\text{CO})(\text{PPh}_3)]$  and iodomethane in acetone.

Integration of equation (5) yields equation (6) with  $[\text{S}] \gg [\text{Rh}(\text{MeCupf})(\text{CO})(\text{PR}_3)(\text{CH}_3)(\text{I})]$ .

$$k_{\text{obs}} = k_4[\text{S}] + k_{-4} = k'_4 + k_{-4} \quad (6)$$

Equation (6) predicts a rate constant which is independent of the iodomethane concentration with an intercept of  $k_{-4}$ .

### 3.5. Kinetic results

The linear dependence between the observed rate constant and the iodomethane concentration at different temperatures is clearly illustrated in Fig. 3 and the values of  $k_1$  and  $k_2$  are reported in Table 2. The  $k_1$  (slope) and  $k_2$  (intercept) values obtained in acetone were also used to calculate the activation enthalpy ( $\Delta^\ddagger H$ ) and entropy ( $\Delta^\ddagger S$ ) using the Eyring equation. The values found for the oxidative addition are 48 kJ/mol for  $\Delta^\ddagger H$ , which is normal for this kind of reaction. For  $\Delta^\ddagger S$  a value of  $-137$  J/K/mol was found, which corresponds with the associative character of the reaction.

The kinetic study of the disappearance and formation of these different complexes in the IR region clearly indicates that the rate of  $\text{Rh}^{\text{I}}$  disappearance ( $2.0(2) \times 10^{-3} \text{ M}^{-1}\text{s}^{-1}$ ) and the rate of  $\text{Rh}^{\text{III}}$ -alkyl formation ( $2.1(5) \times 10^{-3} \text{ M}^{-1}\text{s}^{-1}$ ) are the same within experimental error (Fig. 4). The rate for the formation of the  $\text{Rh}^{\text{III}}$ -acyl product is approximately a factor 13 slower than the above mentioned reactions.

The rate of  $\text{Rh}^{\text{III}}$ -acyl formation was also found to be  $[\text{CH}_3\text{I}]$  independent with an average rate constant of  $1.5(9) \times 10^{-3} \text{ M}^{-1}\text{s}^{-1}$  (Fig. 4). From these discussions it is clear that there is a fairly good correlation between the mechanism and the subsequent rate laws for this system and the experimental results that were obtained in

Table 2  
Solvent effect for the oxidative addition of  $[\text{Rh}(\text{MeCupf})(\text{CO})(\text{PPh}_3)]$  with iodomethane at 25.0 °C using UV/visible spectroscopy  $k_2 = k'_2/[\text{S}]$ .

Solvent	$\epsilon$ [11]	$D$ [11]	$10^3 k_1 (\text{M}^{-1} \text{s}^{-1})$	$10^4 k_2 (\text{s}^{-1})$	$10^5 k_2 (\text{M}^{-1} \text{s}^{-1})$	$k_1/k_2$
Benzene	2.3	0.1	0.101(2)	0.02(1)	0.0178	567
Ethyl acetate	6	17.1	0.658(7)	0.94(3)	0.919	71
Acetone	17	17	1.33(4)	5.1(2)	3.75	35
Chloroform	4.8	4	2.31(2)	8.5(1)	6.8	33
Methanol	32.6	19	3.94(5)	12.0(3)	4.86	81
Acetonitrile	38	29.8	5.18(6)	15.7(4)	8.2	63

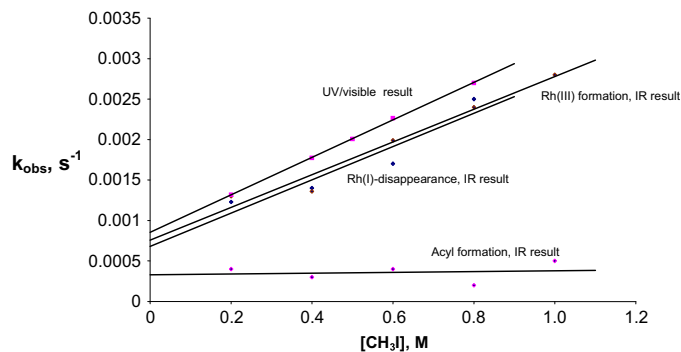


Fig. 4. Comparison between IR and UV kinetic results for the reaction between  $[\text{Rh}(\text{MeCupf})(\text{CO})(\text{PPh}_3)]$  and iodomethane in chloroform at 25.0 °C.

this study. This suggests that the model presented in Scheme 3 is a fair reflection of the reaction that was experimentally investigated.

The UV/visible spectra on the other hand only showed one reaction in the wavelength range that was used. All these spectra showed a steady absorption increase at about 400 nm. The kinetic results for the reaction between  $[\text{Rh}(\text{MeCupf})(\text{CO})(\text{PR}_3)]$  with iodomethane in chloroform (same conditions as those of the IR study) gave a rate constant of  $2.31(3) \times 10^{-3} \text{ M}^{-1}\text{s}^{-1}$ , which corresponds very favourably with the rate constants for  $\text{Rh}^{\text{I}}$  disappearance and  $\text{Rh}^{\text{III}}$ -alkyl formation. It is difficult to assign the UV/visible spectrum change to either the  $\text{Rh}^{\text{I}}$  disappearance or  $\text{Rh}^{\text{III}}$ -alkyl formation due to the fact that the two rate constants are virtually the same. The absence of a second reaction in the UV/visible area can be attributed to a very small extinction coefficient for the acyl product as well as its rate of formation being slow compared to that of the oxidative addition reaction.

The UV/visible kinetic study for a whole temperature range as well as the IR kinetic study gave straight lines with relatively large intercepts as predicted by equation (3). The fact that the IR spectrum clearly indicates the absence of an equilibrium for the  $\text{Rh}^{\text{I}}$  and  $\text{Rh}^{\text{III}}$ -alkyl reaction (disappearance of  $\nu(\text{CO})$  at  $1978 \text{ cm}^{-1}$ ) leads to the interpretation of the intercept as indicative of a solvent assisted pathway. The kinetics of the same reaction in different solvents clearly pointed to a large difference in rate (slope) as well as solvent pathway intervention (intercept), with the largest contribution by acetonitrile.

A quite significant solvent effect is evident from the values for  $k_1$ , which shows an increasing trend with increased solvent polarity, with chloroform being the only exception (Table 2). The significant solvent dependence of  $k_1$  strongly suggests a mechanism in which a polar transition state is stabilised by more polar solvents and can be taken as evidence that the function of the solvent is to ease the charge separation during the rearrangement and formation of the 5-coordinate intermediate. This idea is also supported from the large entropy of activation for the acetone medium. The relative small  $\Delta^\ddagger H$  values, accompanied by large negative  $\Delta^\ddagger S$  values, indicate an associative mechanism including bond formation and/or partial charge creation (electrostriction) during the formation of the transition state.

Van Eldik et al. [12] conducted a combined solvent, temperature and pressure dependence study on the oxidative addition of

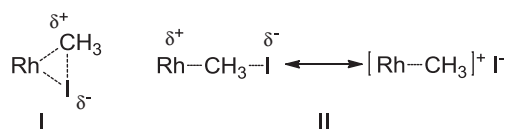


Fig. 5. Representation of a three-centre transition state (I) and linear transition state (II).

[Rh(Sacac)(CO)(PPh<sub>3</sub>)] (Sacac = thioacetylacetonate) and [Rh(Cupf)(CO)(PPh<sub>3</sub>)] with iodomethane. Kinetic data for the [Rh(Sacac)(CO)(PPh<sub>3</sub>)] complex exhibited no significant dependence on the solvent and were interpreted in terms of a concerted three-centre transition state (I) (Fig. 5). The [Rh(Cupf)(CO)(PPh<sub>3</sub>)] complex on the other hand, showed a significant solvent effect in most polar solvents. This observation was interpreted in terms of a linear transition state with participation of an ion-pair intermediate (II).

In order to make a more realistic comparison between the  $k_1$  and  $k_2$  values, the latter was divided by the solvent concentrations to obtain the second order constants,  $k_2$ . The ratio  $k_1/k_2$  is thus a measure of competition between direct CH<sub>3</sub>I addition and solvent dependent pathways. In the case of acetonitrile, the  $k_2$  path becomes more pronounced when compared to  $k_1$  if compared with benzene for example (Table 2). On the other hand, for ethyl acetate and acetone, having nearly the same donicity, the ratio increases almost twofold. The proposed rate-determining  $k_2$  path is exactly the same as that for the solvent dependent path of square planar substitution reactions. The rate of oxidative addition ( $k_1$ -path) changes with a factor of about 51 as the polarity of the solvent increases from benzene to acetonitrile. Highly polar solvents favour the solvent route ( $k_2$ -path) since a factor 785 increase was found for the  $k_2$ -path while only a factor of 51 was noticed for the  $k_1$ -path.

The increase in the  $\sigma$ -donating ability of tertiary phosphines by the introduction of electron donating substituents must always be considered in conjunction with the effect that electron donating groups will have on the  $\pi$ -backbonding capabilities of the phosphine. This is especially true when tertiary phosphines are used as ligands in transition metal complexes, since their electron donor–acceptor capabilities determine the electron density on the metal and this will have an effect on other possible ligands such as CO. The metal centre acts as a nucleophile when a transition metal complex undergoes oxidative addition reactions. The ability of a ligand to increase the electron density on the central metal, will lead to an increase in the rate of oxidative addition, assuming all other influences, factors and parameters remain constant. The oxidative addition of [Rh(MeCupf)(CO)(PR<sub>3</sub>)] with iodomethane illustrates the steric and electronic effect of tertiary phosphines on the rate of oxidative addition.

According to Table 3, the first three phosphines are isosteric with a common Tolman cone angle of 145° and therefore have the same steric demand on the expected rate. However, electronically there is an increase in their  $\sigma$ -donating ability as predicted by their respective Brønsted  $pK_a$  values [13]. The second-order rate constants for the oxidative addition ( $k_1$ ) show a corresponding increase from PPh<sub>3</sub> to P(*p*-MeO-Ph)<sub>3</sub>. This is in agreement with the higher nucleophilicity of the respective Rh<sup>I</sup> complexes. In accordance, the  $k_1$  path shows a 5 fold increase from PPh<sub>3</sub> to P(*p*-MeOC<sub>6</sub>H<sub>4</sub>)<sub>3</sub> which is an expected trend for a nucleophilic attack at the sp<sup>3</sup> carbon of iodomethane. The result  $k_1(\text{PCy}_3) > k_1(\text{P}(o\text{-Tolyl})_3)$  is in agreement with the electronic effect. The fact that both values are less than that of P(*p*-MeOC<sub>6</sub>H<sub>4</sub>)<sub>3</sub> indicates that the steric effect is also operative. However, upon considering the  $pK_a$  value of

**Table 3**

Ligand effect for the oxidative addition of [Rh(MeCupf)(CO)(PR<sub>3</sub>)] with iodomethane at 25.0 °C using UV/visible spectroscopy in acetone. The  $\nu_{\text{CO}}$  values are from this study, the  $pK_a$  values are those of the free phosphines, and the cone angles those of Tolman [10].

PR <sub>3</sub>	$pK_a$	$\nu_{\text{CO}}$ (cm <sup>-1</sup> )	Cone angle (°)	10 <sup>3</sup> $k_1$ (M <sup>-1</sup> s <sup>-1</sup> )	10 <sup>4</sup> $k_2'$ (s <sup>-1</sup> )
PPh <sub>3</sub>	2.73	1982	145	1.33(4)	5.1(2)
P( <i>p</i> -Tol) <sub>3</sub>	3.84	1970	145	2.30(7)	3.5(3)
P( <i>p</i> -MeOC <sub>6</sub> H <sub>4</sub> ) <sub>3</sub>	4.57	1964	145	7.05(7)	7.89(4)
PCy <sub>3</sub>	9.65	1954	170	3.35(4)	5.2(2)
P( <i>o</i> -Tol) <sub>3</sub>	3.08	1965	194	0.615(5)	2.55(3)

**Table 4**

Kinetic data for the oxidative addition of selected [Rh(LL'-BID)(CO)(PPh<sub>3</sub>)] complexes with iodomethane in chloroform at 25.0 °C.

L-L'-BID	L	L'	Ring size	Rate constants		Ref.
				Alkyl (M <sup>-1</sup> s <sup>-1</sup> )	Acyl (s <sup>-1</sup> )	
Cupf	O	O	5	0.0050(1)	0.0012(1)	[1c]
MeCupf	O	O	5	0.00231(2)	0.00015(9)	This work
acac	O	O	6	0.0065(4)	0.0016(1)	[15]
Sacac	O	S	6	Not observed	>0.01	[16]
hpt	O	S	5	0.0083	0.01	[17]
macsm	N	S	6	0.034(1)	0.0078(4)	[18]

PCy<sub>3</sub> (9.65), it is anticipated that  $k_1$  for PCy<sub>3</sub> should be larger compared to P(*p*-MeOC<sub>6</sub>H<sub>4</sub>) (pK<sub>a</sub> of 4.57). Since the cone angle of PCy<sub>3</sub> is 170°, it has a much larger steric demand compared to PPh<sub>3</sub>, P(*p*-Tol)<sub>3</sub> and P(*p*-MeOC<sub>6</sub>H<sub>4</sub>)<sub>3</sub> (145°), and the electronic effect is overshadowed by the steric component resulting in a  $k_1$  value of only 0.00335(4) for PCy<sub>3</sub>. This is approximately a twofold decrease when compared to P(*p*-MeO-Ph)<sub>3</sub>.

A reaction mechanism consistent with the experimental results is shown in Scheme 3. The  $k_1$  path implies a nucleophilic attack on iodomethane giving the 5-coordinate intermediate for which the degree of ion separation will be solvent dependent. During the Rh–CH<sub>3</sub> bond formation, the CH<sub>3</sub> ligand will tend, based on similar assumptions for square-planar substitution reactions [14] to move towards the least strongly bound ligand (nitroso oxygen) and away from the most strongly bound ligand (PPh<sub>3</sub>). Once the Rh–C bond is established, the phosphorus atoms can facilitate the simultaneous C–I bond breaking. The same effect will also facilitate the fast nucleophilic attack of I<sup>-</sup> between the Rh–C and Rh–O bonds thus leading to the proposed *cis*-addition product [1c].

The rate of the oxidative addition of [Rh(MeCupf)(CO)(PPh<sub>3</sub>)] with iodomethane is slightly faster than that of the corresponding [Rh(Cupf)(CO)(PPh<sub>3</sub>)] complex (Table 4), but still appreciably slower than the six-membered [Rh(acac)(CO)(PPh<sub>3</sub>)] complex. The electronic effect of the addition of a methyl group to the cupferron backbone in the current structure is relatively small. From these results it appears that the methyl group donates electron density to the bidentate ligand. This in turn increases the electron density on the rhodium centre which renders the metal complex to be a better Lewis base. The final result is better interaction between the metal d-orbital and the  $\sigma^*$ -orbital of the iodomethane and finally an increase in the oxidative addition rate (bond breaking of the CH<sub>3</sub>–I bond).

The data in Table 4 indicate that in general, for the same donor atoms L and L', an increase in the rate of oxidative addition with an increase in size of the chelate ring is observed. The increase in rate of oxidative addition, correlating to the donor atoms of the bidentate ligands, is found to be in the order O,O < O,S < O,N < N,S while no meaningful correlation was found for the rate of acylation.

#### 4. Conclusions

Sterically and electronically different rhodium(I) complexes bearing the 2-methyl substituted MeCupf ligand have been synthesised and fully characterised. It appeared that in the substitution of one carbonyl ligand for a tertiary phosphine, a mixture of two isomers was formed. In contrast to earlier reports, this appears to be a general reaction pattern for this type of ligand. The oxidative addition of iodomethane to the monophosphine complexes was exhaustively investigated. From these studies it was concluded that there is only a forward reaction in the oxidative addition, with no observed reverse reaction. The subsequent carbonyl insertion was

relatively slow. A large solvent effect was observed for the more polar solvents, indicating that a solvento-species is involved on those occasions. In addition to the electronic effect, the steric influence of these monodentate donor ligands cannot be underestimated. Apparently, the steric bulk introduced by the phosphine substituents hampers the approach of the incoming iodomethane, lowering the rate of oxidative addition. This shows that an optimum exists for the propensity of oxidative addition for this type of complexes, with a fine balance to strike between electron donating groups and steric bulk.

## Acknowledgements

Financial assistance from the South African National Research Foundation (NRF), THRIP and Research Fund of the University of the Free State is gratefully acknowledged. Opinions, findings, conclusions or recommendations expressed in this material are those of the authors and do not necessarily reflect the views of the NRF.

## References

- [1] (a) S.S. Basson, J.G. Leipoldt, J.T. Nel, *Inorg. Chim. Acta* 86 (1984) 167–172; (b) S.S. Basson, J.G. Leipoldt, A. Roodt, J.A. Venter, T.J. van der Walt, *Inorg. Chim. Acta* 119 (1986) 35–38; (c) S.S. Basson, J.G. Leipoldt, A. Roodt, J.A. Venter, *Inorg. Chim. Acta* 128 (1987) 31–37; (d) S.S. Basson, J.G. Leipoldt, J.T. Nel, *Inorg. Chim. Acta* 84 (1987) 167; (e) J.G. Leipoldt, S.S. Basson, L.J. Botha, *Inorg. Chim. Acta* 168 (1990) 215–220; (f) J.G. Leipoldt, E.C. Steynberg, R. van Eldik, *Inorg. Chem.* 26 (1987) 3068–3070; (g) G.J. van Zyl, G.J. Lamprecht, J.G. Leipoldt, T.W. Swaddle, *Inorg. Chim. Acta* 143 (1988) 223–227; (h) J.G. Leipoldt, G.J. Lamprecht, G.J. van Zyl, *Inorg. Chim. Acta* 96 (1985) L31–L34; (i) D.M.C. Smit, S.S. Basson, A. Roodt, E.C. Steynberg, *Rhodium Express* 7–8 (1994) 12–16; (j) Y.M. Terblans, S.S. Basson, W. Purcell, G.J. Lamprecht, *Acta Crystallogr.* C51 (1995) 1748–1750; (k) P. Ebenebe, S.S. Basson, W. Purcell, *Rhodium Express* 16 (1996) 11–16; (l) M. Theron, E. Grobbelaar, W. Purcell, S.S. Basson, *Inorg. Chim. Acta* 358 (2005) 2457–2463; (m) E. Grobbelaar, W. Purcell, S.S. Basson, *Inorg. Chim. Acta* 359 (2006) 3800–3860; (n) J. Conradie, G.J. Lamprecht, A. Roodt, J.C. Swartz, *Polyhedron* 23 (2007) 5075–5087; (o) M.M. Conradie, J. Conradie, *Inorg. Chim. Acta* 361 (2008) 2285–2295; (p) J. Conradie, J.C. Swartz, *Organometallics* 28 (2009) 1018–1026; (q) A.J. Muller, J. Conradie, W. Purcell, S.S. Basson, J.A. Venter, *S. Afr. J. Chem.* 63 (2010) 11–19; (r) M.M. Conradie, J. Conradie, *Dalton Trans.* 40 (2011) 8226–8237.
- [2] S.S. Basson, J.G. Leipoldt, J.A. Venter, *Acta Crystallogr.* C46 (1990) 1324–1326.
- [3] K.G. van Aswegen, J.G. Leipoldt, I.M. Potgieter, G.J. Lamprecht, A. Roodt, G.J. van Zyl, *Transition Met. Chem.* 16 (1991) 369–371.
- [4] L.J. Damoense, Ph.D. Thesis, Unpublished Results, Univ. of the Free State, Bloemfontein, South Africa, 2000.
- [5] Scientist for Windows, Least Square Parameter Estimation, Version 4, Micro-math, 1990.
- [6] J.A. McCleverty, G. Wilkinson, *Inorg. Synth.* 28 (1990) 84–86.
- [7] A.T. Balaban, R.E. Garfield, M.J. Lesko, W.A. Seitz, *Org. Prep. Proced. Int.* 30 (1998) 439–446.
- [8] M. Ahmed, A.J. Edwards, C.J. Jones, J.A. McCleverty, A.S. Rothin, J.P. Tate, *Dalton Trans.* (1988) 257–263.
- [9] S.S. Basson, J.G. Leipoldt, W. Purcell, J.A. Venter, *Acta Crystallogr.* C48 (1992) 171–173.
- [10] C.A. Tolman, *Chem. Rev.* 77 (1977) 313–348.
- [11] U. Mayer, V. Gutman, *Adv. Inorg. Chem. Radiochem.* 17 (1975) 189–230.
- [12] R. van Eldik, J.G. Leipoldt, J.A. Venter, *Inorg. Chem.* 30 (1991) 2207–2209.
- [13] C.A. McAuliffe, G. Wilkinson, *Comprehensive Coordination Chemistry*, Pergamon Press, New York, 1987, p. 989.
- [14] K.F. Purcell, J.C. Kotz, *Inorganic Chemistry*, Saunders College Publishing, Philadelphia, 1977, p. 392.
- [15] D.E. Graham, G.J. Lamprecht, I.M. Potgieter, A. Roodt, J.G. Leipoldt, *Transition Met. Chem.* 16 (1991) 193–195.
- [16] Y. M. Terblans, M.Sc. Thesis, Unpublished Results, Univ. of the Free State, Bloemfontein, South Africa, 1993.
- [17] H. Preston, Ph.D. Thesis, Unpublished Results, Univ. of the Free State, Bloemfontein, South Africa, 1993.
- [18] A. Roodt, G.J.J. Steyn, *Recent Res. Dev. Inorg. Chem.* 2 (2000) 1–23.



**Stefan Warsink** (1981) obtained his PhD in 2011 at the University of Amsterdam under the supervision of Prof. C.J. Elsevier. The focus of his dissertation was the synthesis and characterization of palladium NHC complexes and their application in Z-selective transfer hydrogenation of alkynes. From early 2012, he moved to the research group of Prof. A. Roodt at the University of the Free State, Bloemfontein (South Africa) as a Postdoctoral Fellow. His research focuses on rhodium complexes bearing heteroditopic ligands for the carbonylation of methanol and the kinetic studies thereof. He also joined the crystallographic team of the group.



**Faniel Gebremichael Fessha** obtained his MSc in Inorganic Chemistry. He is currently employed as scientist by Life Technologies in the USA. He has years of industry experience in making oligonucleotide and assays and has a great interest in creating and designing protocols for manufacturing processes. He is also involved in the developing and optimizing of synthesis and purification of DNA probes.



**Walter Purcell** has been in the academic environment for the last 25 years and obtained his PhD in Inorganic Chemistry. He has been promoter and co-promoter for a number of Masters and Ph.D. students in both Analytical and Inorganic Chemistry. He has numerous articles in international journals and also contributed a number of papers at national and international conferences. His research interest includes the study of the reaction kinetics of organometallic and inorganic substances in organic and water mediums as well as the quantification and identification of different elements in natural minerals and ores, synthesis of organometallic complexes, crystallography, ISO 17025, method development and statistic validation.



**Johan A. Venter** obtained his PhD in Inorganic Chemistry. He specializes in the oxidative addition reactions of organotransition metal complexes. He publishes internationally and presented papers at several conferences, both local and international. His interests are in the platinum group chemistry, organometallic complexes, inorganic synthesis, oxidative addition, reaction kinetics X-ray crystallography and method validation in Analytical Chemistry.